Applied Surface Science 270 (2013) 272–280

Contents lists available at SciVerse ScienceDirect

Applied Surface Science

journal homepage: www.elsevier.com/locate/apsusc

Effect of UV and electrochemical surface treatments on the adsorption and reaction of linear alcohols on non-porous carbon fibre

S. Osbeck[a,1], S. Ward[b], H. Idriss[a,c,*]

[a] Materials Research Centre, School of Engineering, Robert Gordon University, Aberdeen AB10 1FR, UK
[b] Cytec Engineered Materials, The Wilton Centre, Wilton, Redcar TS10 4RF, UK
[c] Department of Chemistry, University of Aberdeen, Old Aberdeen, Aberdeen AB24 3EU, UK

ARTICLE INFO

Article history:
Received 25 September 2012
Received in revised form 8 December 2012
Accepted 27 December 2012
Available online 11 January 2013

Keywords:
Fibre carbon surface
UV/O_3 treatment
Temperature programmed desorption
Linear alcohols reaction
Dehydrogenation and dehydration reactions

ABSTRACT

The adsorption properties of untreated, electrochemically treated and ultra-violet/ozone treated polyacrylonitrile based carbon fibres were investigated using temperature programmed desorption (TPD) on a series of linear alcohols as probes in order to understand its surface properties. Surface uptake was found to be sensitive to both the surface treatment and the nature of the adsorbates. Surface coverage increased with increasing alcohol chain due to the increase in their polarizability. It also increased with the level of surface oxygen of the fibres most likely because it facilitates the O—H bond dissociation of the alcohol functional group. In addition, the desorption temperature (during TPD) tracked the surface oxygen levels (as determined from XPS O1s signal) suggesting increasing in the adsorption energy. The reactions of C1–C4 linear alcohols were also investigated on the surface of the fibre carbon. The main reaction was dehydrogenation to the corresponding aldehydes; the dehydration reaction to olefins was not observed. The dehydrogenation reaction was sensitive to the length of the alky chain. It was highest for methanol (to formaldehyde) and decreased with increasing the carbon number. Overall TPD of linear alcohols was shown to be a promising method for quantifying the level and strength of bonding occurring on carbon fibre surfaces.

1. Introduction

Carbon fibre composites are widely used in the aerospace industry due to their favourable strength to weight ratio [1]. While there have been many investigations into the correlation between the surface functional groups on the carbon fibre and the resin matrix components, the exact nature of the relationship is still not fully understood [2]. Fibres are often mixed with a resin matrix, making a composite material, to increase its strength. The composite strength depends on several factors chief of them the stress transfer between the fibre and the resin which is largely dependent on their interfacial bonding. Adsorption is considered one of the major theories to explain adhesion [3]. Many methods have been designed to functionalise the surface of carbon so adhesion to the resin is increased. These include acid treatment [4], γ-ray radiation [5], UV radiation [6], and thermochemical methods [7]. Like all surfaces, reactions do not occur across the entire carbon surface but instead occur at discrete sites where the valency is not satisfied. In the case of carbon, these sites include edges of basal planes, twin boundaries, and imperfections such as vacancies, dislocations and impurity sites (e.g. oxygen functionalities) [8]. Temperature programmed desorption (TPD) has been used previously to determine the functional groups present on carbon fibres and activated carbons [9–14]. It has also been used to determine the adsorption of volatile organic compounds on fibres and activated carbons [15,16]. TPD has not yet been used to examine adsorption on non-porous carbon fibres due to its lower surface area, typically about 1 m^2/g.

TPD reactions of alcohols are extensively used to study surface reactions of metal [17,18] and metal oxide [19], metal carbides [20], and metal/metal oxides [21,22] materials among others. In general there are two modes of adsorption; molecular (RCH_2OH (a)) and dissociative adsorption ($RCH_2O(a) + H(a)$). Molecular adsorption often occurs at lower temperatures than dissociative adsorption and is often found on metallic systems as well as on surfaces with a degree of covalent bonding between atoms. For more ionic systems and in particular in the presence of surface oxygen, where the electronic density is more localised on the surface metal anions, dissociative adsorption is predominant. Adsorption energies of these compounds are also extensively studied. In general, the dissociative adsorption leading to alkoxides and hydroxyls is more favoured

* Corresponding author. Current address: Saudi Basic Industries Corporation, P.O. Box 42503, Riyadh 1151, Saudi Arabia. Tel.: +966 1 499 9738; fax: +966 1 499 9101.
E-mail addresses: h.idriss@abdn.ac.uk, idrissh@sabic.com, h.idriss@auckland.ac.nz (H. Idriss).
[1] Current address: Sonomatic Ltd., Unit 1, Energy Development Centre, Claymore Drive, Bridge of Don, Aberdeen, AB23 8GD, UK.

0169-4332
http://dx.doi.org/10.1016/j.apsusc.2012.12.173

Table 1
Fragmentation patterns of the series of alcohols used. The main mass fragment of interest is highlighted in bold.

Probe	*m*/*z*															
	15	26	27	28	29	**31**	39	41	42	43	45	55	56	59	60	74
Methanol	12	–	–	5	45	**100**	–	–	–	–	–	–	–	–	–	–
Ethanol	7	10	22	3	30	**100**	–	1	5	11	51		–	–	–	–
1-Propanol	2	6	16	6	18	**100**	7	9	14	4	2	1	–	11	7	–
1-Butanol	10	14	57	20	38	**98**	25	88	43	68	8	28	100	–	–	1

than the molecular adsorption, although both may co-exist on the surface.

In a previous work [23] we have investigated in some detail, using electron spectroscopy, the concentration of surface oxygen atoms on carbon fibres after chemical treatment as well as UV/O_3 treatment. It was found that UV/O_3 treatment resulted in a greater degree of surface oxidation when compared to conventional electrochemical treatment. In order to gauge the effect of these treatments on the surface adhesion of these non-porous carbon fibres we have studied the adsorption and reaction of a series of linear alcohols using a highly sensitive TPD set up (due to the low surface area of the carbon fibre) to track the reaction products.

2. Materials and experimental

2.1. Fibres

High strength, intermediate modulus, unsized PAN based carbon fibres provided by Cytec Engineered Materials Ltd. (Wilton, UK) were used in this study. Untreated fibres (U) were examined. Various levels of surface oxygen were achieved through electrochemical treatments (0.2B, 3B, 6B and 3A) and an ultraviolet/ozone (UV/O_3) treatment as described previously [23]; B stands for base treatment and A for acid treatment and the preceding number is an indication of the charge applied to the treatment. The standard setting was not investigated as it is proprietary knowledge. UV/O_3 fibres were treated as long tows for 4 h in a Jelight UVO cleaner/oxidiser; Model 42-220 (Jelight Company Inc., California, USA) and were turned regularly to achieve all over treatment.

2.2. Fibre characterisation

Surface oxygen levels (%) were determined by X-ray photoelectron spectroscopy (XPS) and functional groups were characterised by peak fitting. XPS measurements were made on a Kratos Axis HSi spectrometer at a residual vacuum of 10^{-7} Pa, using a monochromatic Al K_α source (energy 1486.6 eV). Narrow scans (pass energy = 20 eV) for C1s, O1s, N1s and Si2p were performed three times and averaged at three positions on each sample. The average surface composition was determined from the area beneath the elemental peaks following a Shirley background subtraction and using relevant empirical atomic sensitivity factors; C1s (0.25), O1s (0.66), N1s (0.42), Si2p (0.23) and Na1s (2.3) (Kratos Analytical Ltd., Manchester, UK). Curve fitting was performed using XPSPEAK 4.1 (Dr Kwok, Chinese University of Hong Kong). The G/L mix was fixed to 0.2 for the graphite peak and 0.5 for all the others. Peak shifts were fixed in relation to the graphite peak. UV/O_3 treated fibres were placed in the XPS vacuum directly after treatment. Surface morphology of all the fibres was examined by scanning electron microscopy (SEM). The fibre structure was investigated using transmission electron microscopy (TEM).

2.3. Temperature programmed desorption

The TPD set up consisted of a U shaped quartz glass reactor bed, a vacuum system, a furnace, a temperature controller, and a mass spectrometer. The vacuum was provided by a Duoseal rotary vane pump (WM Welch Manufacturing Company, Chicago, USA), and a vapour diffusion pump (Edwards, West Sussex, UK, model number EO2) backed by an Edwards 5 vane rotary pump (model number E2M5). The base pressure in the system was typically 4×10^{-5} Pa. Pressures were measured using a Dynavac model CG8 cold cathode gauge (Dynavac Engineering Pty. Ltd., Victoria, Australia). The temperature of the glass lined furnace was monitored using a K type thermocouple and was ramped by a Kaif digital temperature controller (Kaif Digital, Arizona, USA) at a linear rate of 20 K/min. The thermocouple was placed as close to the sample as possible in order to get accurate temperature readings of the sample. The mass spectrometer was a Spectra Vision quadrupole (LEDA Mass Ltd., Cheshire, UK) with a capability of measuring 12 masses simultaneously in the range 1–200 amu.

Long lengths of carbon fibres, weighing between 0.4 and 0.7 g were packed into the reactor. The fibres were degassed at 150 °C (423 K) for 2 h to remove any physisorbed gases. The system was allowed to cool and 1 μL of methanol, ethanol, 1-propanol or 1-butanol (purity > 99%) was then injected into the system via the dosing line at room temperature with the sample isolated from the vacuum system. The sample and the injected alcohol were allowed 15 min to come to equilibrium before any excess was pumped out. The fibres were degassed until the pressure reached approximately the pre-dosing level. The temperature of the system was then raised from room temperature to 450 °C (723 K) and the appropriate mass fragments for each alcohol were monitored. Table 1 lists the fragmentation patterns for the alcohols used in this study [24]. The main mass fragment of interest is *m*/*z* 31 (parent ion $-CH_2OH^+$).

Peak areas for the *m*/*z* 31 spectra were calculated by integrating the area under the peak using the trapezoid rule after applying a linear background subtraction. A correction factor appropriate to the adsorbed alcohol was then applied with respect to *m*/*e* 31; 2.4 for methanol and ethanol, 1.5 for propan-1-ol, and 4.7 for butan-1-ol. The correction factor accounts for ionisation efficiency, mass fragment yield for the desorbing particles, quadrupole transmission, and electron multiplier gain of the mass spectrometer [25]. Table 2 presents the number of moles in 1 μL of liquid for the series

Table 2
Molecules of probe in 1 μL of liquid and computed radius.

Liquid	Density (kg/m^3)	Moles	Molecules	Radius[a] (nm)
Methanol	786.5	2.46×10^{-5}	1.5×10^{19}	0.22
Ethanol	785.1	1.71×10^{-5}	1.0×10^{19}	0.26
n-Propanol	800.0	1.33×10^{-5}	8.0×10^{18}	0.29
n-Butanol	809.7	1.09×10^{-5}	6.6×10^{18}	0.31

[a] Computed radius of alcohol molecules using B3LYP density functional theory (DFT) with 631 + G* basis set as implemented by the Spartan 08 code.

Table 3
Functional groups on fibres as determined by XPS C1s where A and B represent the acid and base treatments respectively, and UV/O_3 the ultraviolet ozone treatment.

Treatment	%					
	U	0.2B	3B	6B	3A	UV/O_3
Graphite (~284.6 eV)	74.8	73.5	73.3	73.4	75.6	64.9
Alkoxide/phenolic/ether (285.8 eV)	14.2	14.5	14.9	16.0	13.8	17.7
Carbonyl/quinine (287.2 eV)	4.1	4.5	5.1	5.2	4.0	6.6
Carboxyl/ester (288.8 eV)	2.9	3.0	3.3	3.6	3.0	8.0
Carbonate (290.6 eV)	1.4	2.3	0.9	1.2	1.1	1.0
Plasmon (291.2 eV)	2.6	2.3	2.4	0.7	2.6	1.9
Carbon[a]	94.8	93.1	89.6	86.7	89.2	73.9
Oxygen	2.4	4.0	7.9	11.4	8.5	21.9

[a] Nitrogen and silicon were also present but are not listed.

of alcohols used. Because the surface area of the carbon fibre is about 1 m^2/g and a densely packed carbon hexagonal structure with 0.25 nm carbon to carbon distance contains about 5×10^{18} sites/g (one site is taken as half the total number of surface carbon sites because the van der Waals radius of the adsorbed alcohol is larger than the 0.25 nm distance), the number of alcohol molecules used is enough for surface saturation. In other words the analysis of the results will assume that surface coverage is not affected by the amount of molecules exposed prior to TPD.

2.4. SEM and TEM

SEM images were acquired for all treated and untreated fibres using a Leo S430 electron microscope (Zeiss, Nano Technology Systems Division, Cambridge, UK). The microscope uses a semiconductor detector for backscatter collection and an Everhart–Thornley detector coupled to a photomultiplier tube for secondary electron detection. The Leo S430 can provide a maximum resolution of approximately 50 nm. Fibres samples were attached to a stainless steel stub using a carbon tab. It was not necessary to sputter coat the samples. Fibres were degassed to approximately 10^{-3} Pa. A spacer bar was used to reduce the working distance to ~10 mm or less. Images were acquired at various magnifications for fibres. TEM images were recorded on a JEOL JEM-2011 high resolution (HR) TEM (JEOL Ltd., Tokyo, Japan). The electrons were produced by a LaB_6 crystal and accelerated up to 200 kV. The TEM is capable of producing a beam diameter as small as 0.5 nm, with 0.19 nm resolution. Images were recorded on a Gatan 794 CCD camera (Gatan Inc., Pleasanton, California, USA). Fibres were either ground and dispersed in acetone or were set in an Epon resin and ultramicrotomed using a diamond cutter to ~100 nm width. The samples were then placed on the copper mesh grids for analysis.

3. Results

3.1. Fibres characterisation

Table 3 lists the surface oxygen levels determined by XPS on the carbon fibres used in this study; detailed study of the untreated, electrochemically treated and O_3 treated fibre carbon surfaces by XPS, Raman, and krypton adsorption were previously studied [23]. UV/O_3 treatments produced substantial increases in surface oxygen compared to the electrochemical treatments (Fig. 1 gives a representative result of the change of the functional group nature and concentration upon UV/O_3 treatment). BET surface area measurements for the electrochemical treatments showed little difference to the untreated fibres; ~1 m^2/g however the fibres treated with UV/O_3 for 4 h returned a surface area of 6.3 m^2/g using krypton; a substantial increase. Fig. 2a shows a SEM image of untreated carbon fibres; a mix of kidney shape and circular cross sections with a diameter of ~5 μm. There were no visible changes to the analysed SEM images with electrochemical or UV/O_3 treatments compared to the untreated ones. The striations were unaltered and no debris generated. Fig. 2b shows a SEM image of a sheared 6B treated fibre. The internal structure of the fibre shows layers approximately aligned with the fibre axis as would be expected for a PAN fibre.

Table 4
Interlayer spacing from TEM.

	d_{002} (nm)
UST	0.386 ± 0.015
6B 1	0.370 ± 0.017
UV/O_3	0.373 ± 0.019

TEM images of the core and the outer layers of the fibres showed a structure with randomly twisted ribbons of graphene generally aligned to the fibre axis as is typical for PAN fibres [26].

Fig. 3a shows a longitudinal image from the core of a UV/O_3 treated fibre prepared by ultramicrotomy. It is possible to distinguish ribbons of carbon which are generally aligned to the fibre axis. Fig. 3b shows a transverse image of the fibre. The ribbons of graphene have a twisted, random, structure in the radial direction. These images are typical of PAN fibres [26].

Diffraction patterns were generated from the TEM images and the interlayer spacing (0 0 2) was calculated.

Fig. 3c and d shows examples of UST and 6B fibres respectively and their associated diffraction patterns. Table 4 lists the average interlayer spacing taken from several images for the three types of

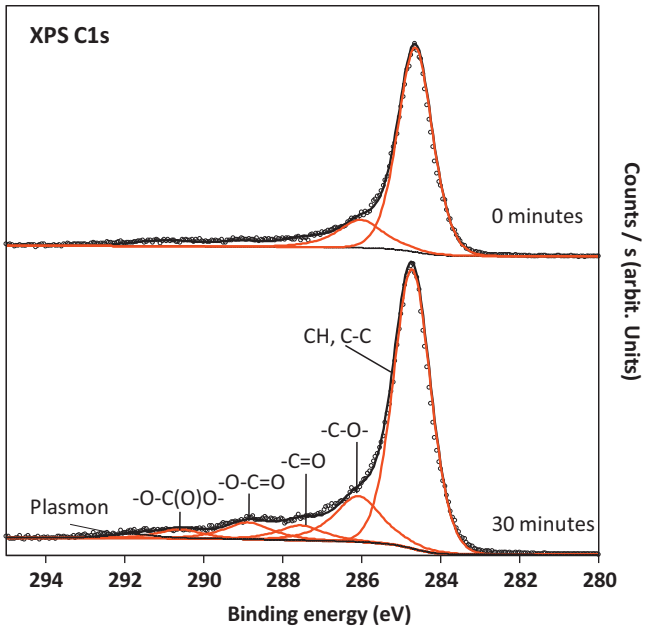

Fig. 1. XPS C1s of carbon fibre before (0 min) and after (30 min) UV O_3 treatment.

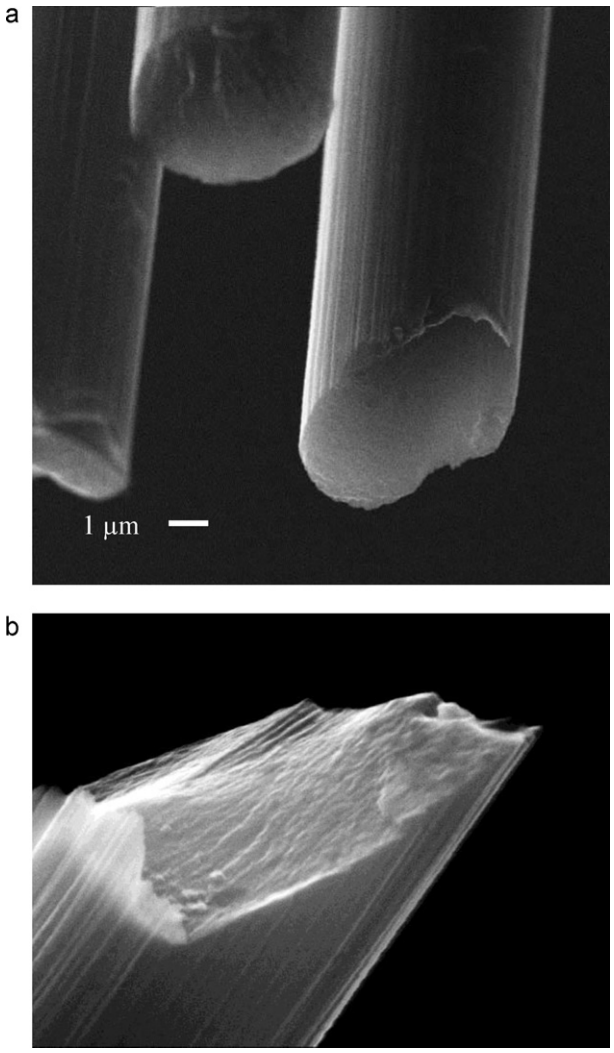

Fig. 2. (a) SEM image (15,000× magnifications, 20 kV) of untreated fibre. (b) SEM image (50,000× magnifications, 20 kV) of 6B treated fibre.

fibres examined. The error quoted represents the 90% confidence interval.

An ideal graphitic material would have an interlayer spacing of 0.335 nm [27]. The fibres therefore display a high level of turbostratic structure. From the error involved in these measurements, it is not possible to tell if there is a difference between fibres. It is unlikely that the treatments would change the internal structure of the fibre, although the BET and XPS suggest the surface layers were altered.

3.2. Reactions with alcohols

Following dosing, the time for degassing varied between 30 min and 2 h depending on the alcohol; butan-1-ol took the longest time to degas. All fibres dosed with an alcohol, showed desorption spectra similar to that shown in Fig. 4. The spectra show two desorption domains. The first domain found at about 450 K consists of masses related to the alcohol (with the parent ion mass of m/z 31 $-CH_2OH^+$) as well as its reaction products. The second desorption above 600 K consists mainly of decomposition products of the functional groups present on the fibre (water (m/z 18), carbon monoxide (m/z 28), and carbon dioxide (m/z 44)). Blank desorption spectra of fibres did not show the first desorption domain. We will focus on the first peak for m/z 31 as it is the most representative of the alcohol–fibre interaction since it is composed exclusively of products resulting from the alcohol desorption/reaction and not from the decomposition of the function groups on the fibre surface. When peak areas are discussed they will refer to peaks in the 450 K region.

Table 5
Mass fragment yield (%) of m/z 29 with respect to m/z 31 for the series of alcohols used on the electrochemically treated fibre carbon.

	Methanol	Ethanol	Propan-1-ol	Butan-1-ol
U	96	40	23	31
3B	121	49	28	33
6B	110	56	31	38
Theoretical	45	30	18	39
Deviation for 6B	65	26	13	−1

Fig. 4 presents the main desorption products of methanol on the 6B fibre. The first domain is composed of methanol and formaldehyde while the second one contains, in addition, decomposition products. In order to understand the reaction, quantitative analysis of masses was conducted. Peak areas were calculated for several mass fragments and the percentage desorbed with respect to m/z 31 was calculated and compared against those of pure molecular desorption. It should be noted that errors due to changes in base pressures between experiments and peak integrations are typically 10–15%. Table 5 shows the results of this calculation for m/z 29 for a selection of the fibres and Fig. 5 shows the trend in the cased of the UV/O_3 fibres. m/z 29 is the main fragment of aldehydes (—CHO) that can be formed by dehydrogenation of the linear alcohol. It can be noted that for methanol, ethanol and propan-1-ol a greater level of desorption of m/z 29 than that provided from the alcohol occurs. Methanol shows the greatest deviation at over twice the percentage expected. Butan-1-ol shows the least deviation, with levels being approximately equal to those of the parent alcohol.

In the case of methanol, formaldehyde is the corresponding aldehyde. A likely formation mechanism of formaldehyde (acetaldehyde) from methanol (ethanol) on an oxidised carbon surface is presented in Eq. (1) and (2), where V_O is an oxygen vacancy, the subscript s represents surface molecules or atoms and the subscript a represents adsorbed molecules or atoms; as a typical oxidative dehydrogenation [28] (similar reactions would occur for the higher alcohols to a lesser extent).

$$CH_3OH_a + C_s - O_s \rightarrow CH_3O - C_s + O_s - H_a \rightarrow HCHO + H_2O + C_s - V_O \quad (1)$$

$$CH_3CH_2OH_a + C_s - O_s \rightarrow CH_3CH_2O - C_s + O_s - H_a \rightarrow CH_3CHO + H_2O + C_s - V_O \quad (2)$$

Methanol showed the greatest degree of aldehyde production. The ratio of measured to expected aldehydes (acetaldehyde from ethanol, propionaldehyde from propanol and butyraldehyde from butanol) decreased with increasing number of carbons in the chain. The driving force for this reaction is the removal of one hydrogen atom and two electrons in the alpha position from the functional group. This hydrogen atom, removed as hydride, will react with the hydroxyl making H_2 that may, in a transition state, react with surface oxygen to give H_2O and leave the two electrons in the lattice to complete the reduction process as described by Eqs. (3) and (4), where the [ ]* indicates a reaction intermediate.

$$CH_3O - C_s + C_s \rightarrow [HC_{(+)}HO - C_s]^* + C_s - H \rightarrow HCHO_{(g)} + C_s + C_s - H \quad (3)$$

$$C_s - H + O_s - H_a \rightarrow [H_2 + C_s - O_s]^* \rightarrow H_2O + C_s + V_O \quad (4)$$

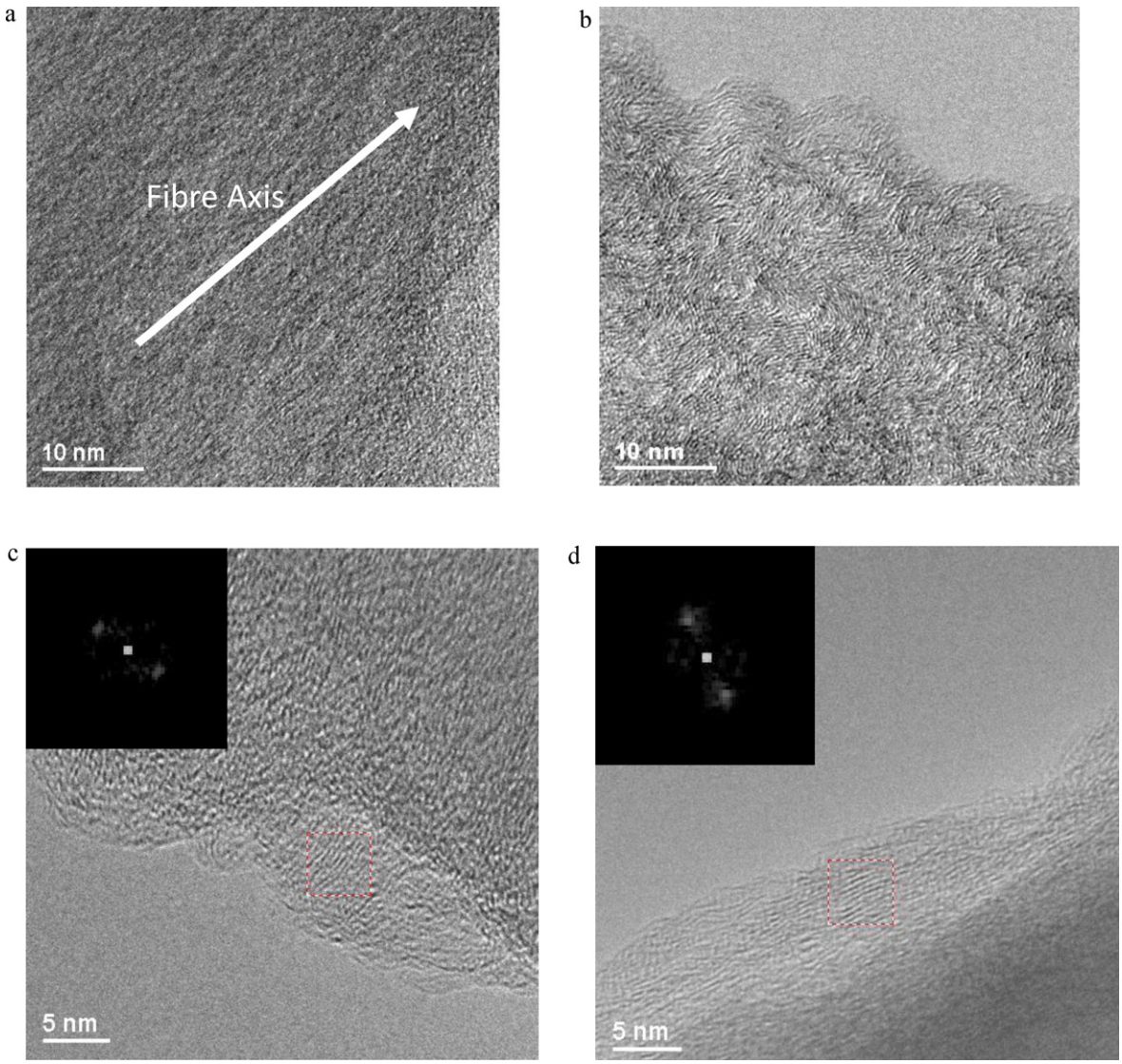

Fig. 3. (a) TEM image of UV/O_3 treated fibre prepared by an ultramicrotome showing the alignment of carbon ribbons to the fibre axis. (b) TEM image of UV/O_3 treated fibre prepared by an ultramicrotome showing the twisted layer structure typical to PAN fibres. (c) TEM image of UST fibre prepared by dispersion and (inset) associated diffraction pattern. (d) TEM image of 6B fibre prepared by dispersion and (inset) associated diffraction pattern.

In the case of methanol all three hydrogen atoms are equivalent, while in the case of ethanol one of them is replaced by $-CH_3$ that in addition to its steric effect will have an inductive effect. As the number of carbons in the molecule increases, i.e. as the structure and charge changes, the probability of dehydrogenation occurring will also change. Figure shows this trend for the UV/O_3 treated fibres. It is clear that increasing the chain, decreases the dehydrogenation reaction. The reason for this might be the decrease of the probability of the surface O2p orbitals to bond with the carbon atom of the alkoxy function when the alkyl chain increases. The other reaction that may also occur is a dehydration reaction to make an olefin, except in the case of methanol where the dehydration reaction may only occur via a bi-molecular interaction to make dimethyl ether. Eq. (5) shows the dehydration reaction for ethanol. The main fragment of interest, m/z 27 ($CH{=}CH_2$), was measured and compared against the theoretically expected percentage. The percentages did not deviate, within experimental errors, from those for the parent molecule suggesting that the dehydration reaction is unfavourable compared to the dehydrogenation reaction.

$$[C_2H_5OH]_a + C_s - O_s \rightarrow [C_2H_5O]_a\,C_s + O_s - H_a \rightarrow C_2H_4 + H_2O + C_s \quad (5)$$

Figs. 6 and 7 show the TPD spectra of m/z 31 for the alcohol series on untreated fibres and fibres treated to 4 h of UV/O_3, respectively. All the TPD curves acquired generally showed similar shapes; broadly symmetric curves with a bias towards higher temperatures. The desorption shape indicates that it is likely to be second order; i.e. re-combinative desorption. In other words, dissociative adsorption occurs at room temperature as generalised in Eq. (6).

$$ROH_{(g)} + O_s\text{-}C_s \rightarrow \text{RO-}C_s + O_s\text{-H at 300 K} \quad (6)$$

Upon heating, energy is given to the adsorbate providing the activation energy needed for the association of H, from O_s-H, to the alkoxide. The tail at high temperature is due to stronger interactions occurring with the surface at lower coverages. This is because at high coverage (low temperature), lateral interactions between adjacent molecules may result in slight destabilisation due to repulsive interactions taking place.

3.3. Effect of surface treatment on alcohols uptake

From Figs. 6 and 7 the following observations can be made. The untreated (U) fibres show very low levels of m/z 31 desorption for methanol and ethanol compared to UV/O_3 treated fibres. As can be

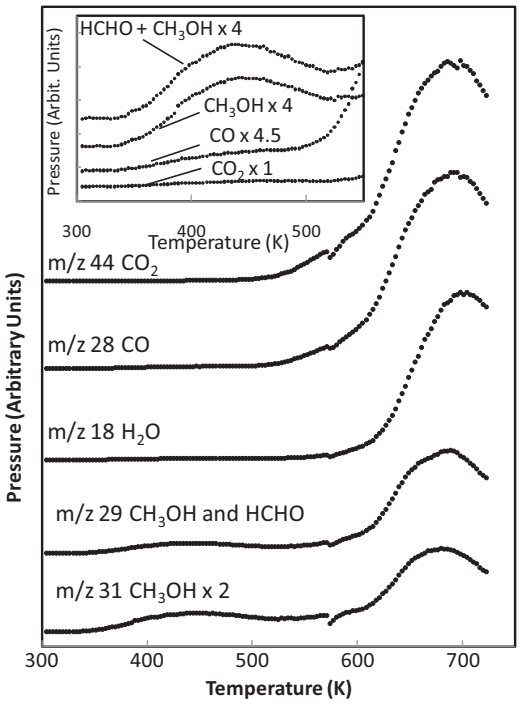

Fig. 4. TPD for methanol on 6B fibres showing selected *m*/*z*. Inset: expanded lower temperature region.

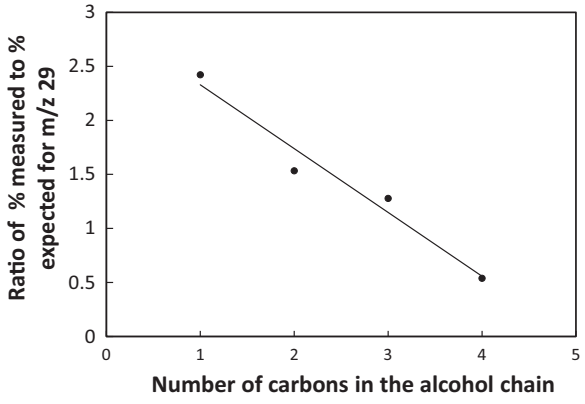

Fig. 5. Ratio of % measured to % expected *m*/*z* 29 with carbon chain length for UV/O_3 treated fibres.

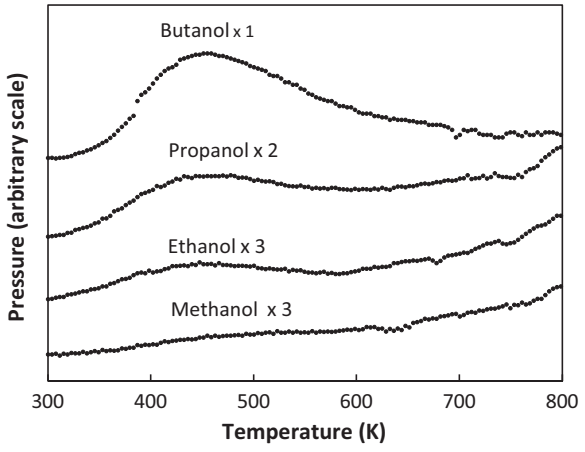

Fig. 6. TPD of a series of alcohols after room temperature adsorption on untreated (U) fibre.

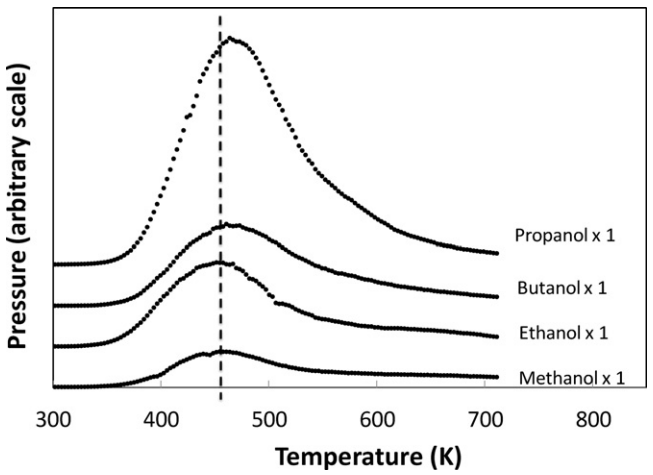

Fig. 7. TPD of the alcohol series C1–C4 for UV/O_3 treated fibres, *m*/*z* 31.

seen for the U fibres the intensity of the *m*/*z* 31 peak for butan-1-ol is greater than the intensity of the other alcohols. The general trend is for larger peaks to occur as the carbon chain in the alcohol increases. Table 6 lists the results for all the fibre and probe combinations. As seen in Table 6, the surface uptake, as monitored by the main desorption fragment of each alcohol, increases with increasing alkyl chain length of the probe. As the alkyl chain increases for an organic molecule, the dipole moment decreases, i.e. the molecule becomes less polar [29]. For liquids, this would result in less polar interactions occurring at the surface and dispersion interactions becoming the dominant force [29]. In the case of gases however, the polarizability of the molecule becomes the most important factor [30].

As the polarizability increases, the acidity also increases, i.e. it becomes easier to dissociate the hydrogen atoms from the molecule. Table 7 lists the polarizabilities of the alcohols used in this study. The polarizability increases linearly with the number of carbons in the molecule. Therefore as the chain length increases, the likelihood of dissociation occurring increases. From Tables 6 and 7 it seems probable that the molecules with longer alkyl chains are being polarised more than those with shorter chains. Since the alcohol molecules on the fibre are only at monolayer coverage, the interactions between the molecules and surface will be dominated by the polarizability and not the dipole moment. There is also a slight shift to higher desorption temperatures with increasing the alkyl chain of this linear alcohols series (up to about 40 K from

Table 6
Integrated peak areas (in arbitrary units) for *m*/*z* 31 for alcohol series per gram of carbon fibre or approximately per m^2 (BET surface area = ca. 1 m^2/g).

	% O	Methanol	Ethanol	Propan-1-ol	Butan-1-ol
U	2.4	8.0×10^{-9}	2.8×10^{-8}	4.8×10^{-8}	7.1×10^{-7}
0.2B	4.0	2.4×10^{-9}	2.0×10^{-8}	7.0×10^{-8}	1.8×10^{-7}
3B	7.9	3.5×10^{-8}	1.3×10^{-7}	3.9×10^{-7}	1.2×10^{-6}
3A	8.5	8.9×10^{-9}	4.4×10^{-8}	4.0×10^{-7}	1.5×10^{-6}
6B	11.4	1.7×10^{-7}	1.3×10^{-7}	4.2×10^{-7}	2.3×10^{-6}
UV/O_3	21.9	7.5×10^{-6}	2.1×10^{-5}	4.3×10^{-5}	4.4×10^{-5}

Table 7
Polarizability of C1–C4 linear alcohols [31].

	Number of carbon atoms	Polarizability (10^{-24} cm^3)
Methanol	1	3.29
Ethanol	2	5.41
Propan-1-ol	3	6.74
Butan-1-ol	4	8.88

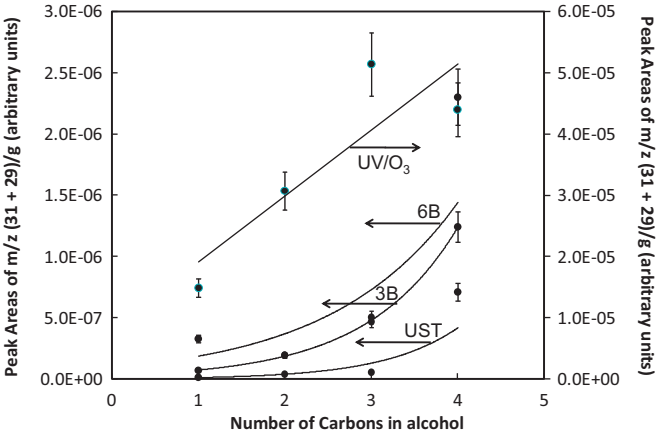

Fig. 8. Peak area of desorbing alcohol (measured by the sum of m/z 31 and m/z 29) per gram of fibre as a function of the number of carbons in the alcohol.

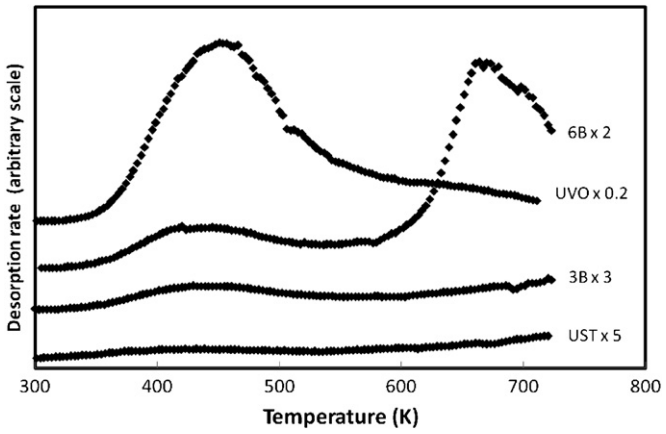

Fig. 9. TPD of m/z 31 from ethanol desorption on U, 3B, 6B and UV/O_3 treated fibres.

methanol to 1-butanol). This is most likely due to stronger adsorption energy of the alkoxide with increasing the number of carbon atoms. These two phenomena (increasing surface population and increasing desorption temperature with increasing number of carbon atoms in the alcohol series) might be related to the increase of their polarizability.

Fig. 8 shows the trends in the peak areas of m/z 31 + m/z 29/g of fibre for the alcohol series on the U, 3B, 6B, and UV/O_3 treated fibres. The untreated and electrochemically treated fibres all showed exponential trends with increasing alkyl chain while the UV/O_3 treated fibres showed a linear trend with chain length. The exponent of the trend lines for the electrochemically-base treated fibres decreases with increasing treatment level suggesting the trend becomes more linear as the oxygen on the fibre increases. While the polarizability of the adsorbate will play a significant part in the amount adsorbed on the fibre, from these figures it seems likely that other factors are influencing the adsorption or desorption. For example, delocalised π-electron rich areas on the carbon basal layers have been found to act as Lewis base sites on carbon catalysts [32,33]. On an oxygen free fibre surface, a background level of adsorption would still occur at the basal sites. As the oxygen level increases on the fibre surface, the number of delocalised π-electrons will decrease and therefore the number of these weak base sites will also decrease. Indeed for the base treated fibres the plasmon level in XPS measurements decreases, as shown in Table 3 suggesting less delocalised electrons. The decrease in weak, background base sites with the increase in strong localised base sites could account for the gradual change from the exponential to linear trend in peak area of m/z 31 with increasing alkyl chain length although further investigation would be of interest.

In addition to alkyl chain length, the peak area of m/z 31 also increased with increasing surface oxygen on the fibre as can be seen in Table 6 and Fig. 9 which shows the TPD spectra of m/z 31 for the untreated fibres and the 3B, 6B, and UV/O_3 treated fibres after dosing with ethanol. The peaks are small for the untreated fibres compared with the 6B fibres; suggesting less adsorption occurs on the untreated fibres. These peaks are much bigger for the UV/O_3 than any other fibre, suggesting even greater uptake of ethanol compared to the electrochemical treatments. This trend was seen for all the alcohol molecules.

Fig. 10a shows the quantity of propan-1-ol desorbed per gram of fibre as a function of surface oxygen. The trend is best described by an exponential curve so the plot is provided on a semi-logarithmic scale. Methanol, ethanol and butan-1-ol showed similar trends.

It is very clear that more alcohol adsorbs on fibres with greater levels of oxygen. Table 3 lists the functional groups on the surfaces

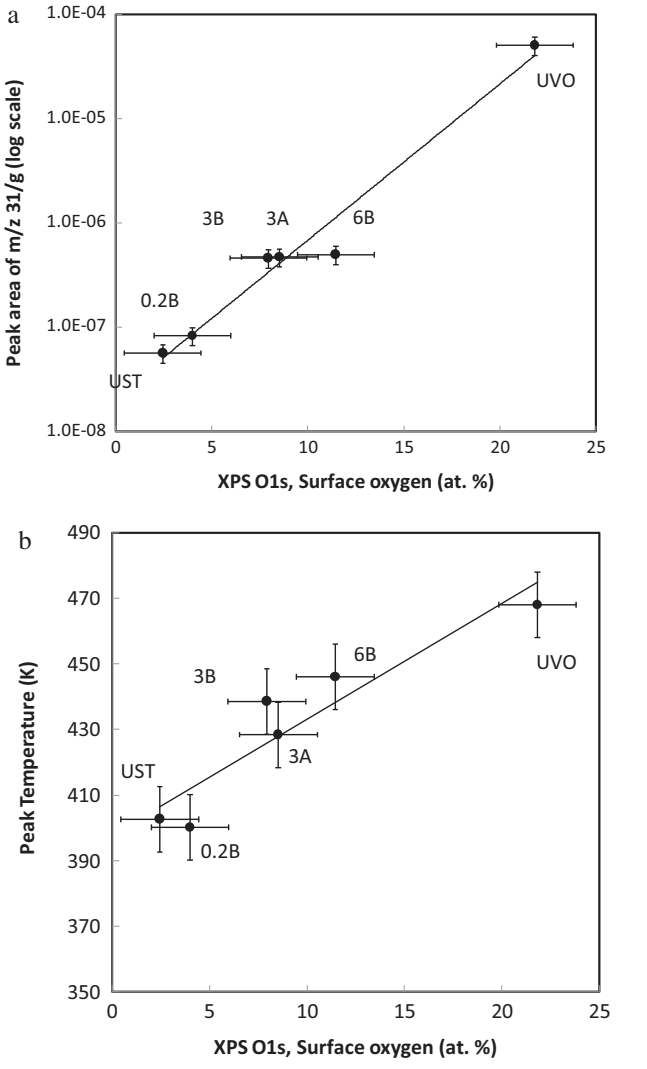

Fig. 10. (a) Semi-logarithmic plot of the peak area of m/z 31 for propan-1-ol desorption (arbitrary units) as a function of surface oxygen. Error bars represent estimated 20% error in peak area measurements and maximum 95% confidence interval for oxygen level. (b) Maximum desorption temperature of propan-1-ol as a function of surface oxygen determined from their corrected XPS O1s signal. Error bars represent estimated ± 10 K error in temperature and maximum 95% confidence interval for oxygen %.

of the fibres used in the TPD experiments as found from the peak fitting performed on the XPS C1s spectra. Plotting the change in the percentage of functional groups against the quantity of m/z 31 desorbed, produces exponential trends for all of the oxygen containing groups with the exception of carbonate which did not show a relationship. One possible reason is that unlike the alkoxides (R-O_s) and carboxylate ($RCOO_a$) groups, the carbonate groups ($OCOO_a$) may not allow for adsorption as they are the most stable.

How strongly the adsorbed species is held on the fibre can be estimated from the temperature of peak desorption. Fig. 10b shows the variation in temperature with level of oxygen present on the fibre surface for propan-1-ol. Butan-1-ol showed a similar trend. This suggests the surface species from propan-1-ol and butan-1-ol adsorption are more tightly bound when there is more surface oxygen present. The trends for methanol and ethanol were less clear.

4. Discussion

The TPD study of the series of C1–C4 linear alcohols on carbon fibres modified by electrochemical and UV/O_3 methods has shown the following four points.

All products desorbed in two temperature domains. The first temperature domain at 450–500 K mainly consisted of the reactant desorption while the second temperature domain (>600 K) mostly consisted of decomposition products (e.g. CO, CO_2, and ketene (m/z 42, 14) among others).

At the low temperature domain, a small fraction of the adsorbed alcohols was dehydrogenated to the corresponding aldehydes. This reaction is very similar to that observed on many oxide surfaces [34–37]. The extent of dehydrogenation was inversely proportional to the number of carbon atoms in the alcohol. The dehydration reaction to olefins was not observed.

The surface uptake showed dependence on the nature of the alcohols; it increased with increasing number of carbon atoms. This increase was co-related to the increase in the acidity of the molecule in the gas phase where the polarizability is the main factor.

The surface uptake also increased with increasing surface oxygen atoms. This was understood as being due to the dissociative adsorption nature whereby two sites are needed: one to accommodate the O atom of the alcohols (surface carbon atom site) and the other to accommodate the hydrogen ion of the alcohol (a surface oxygen site).

The above four points will be discussed taking into account other works albeit on other carbon materials. TPD of alcohols on carbon fibre surfaces has not been reported so there is limited work to compare these results against. Adsorption of volatile organic compounds (VOC) on carbon materials has been investigated using TPD by other workers [15,16]. In a work by Popescu et al. [16], the heats of desorption for toluene and butylacetate were found to be slightly greater than the heat of vaporisation for the pure liquids and therefore the molecules were considered to be physisorbed. The heat of desorption for n-butanol was found to be greater that the heat of vaporisation, however. In one case the enthalpy of desorption was found to be 98.8 kJ/mol; more than twice the enthalpy of vaporisation (43.7 kJ/mol). This suggests a reaction occurred between the adsorbed butan-1-ol and the surface oxygen groups. The authors found aldehydes, particularly formaldehyde (assigned to m/z 31) and butyraldehyde (m/z 72), were produced as well as oxalic acid (m/z 90), formic acid and ethanol (m/z 46) although they concluded further work was required to fully understand the mechanisms involved [16]. The observation of the dehydrogenation pathway is in agreement with the results of this work.

Yi et al. gravimetrically investigated the adsorption of benzene, toluene, methanol, and ethanol on activated carbon fibres [15]. Methanol was seen to adsorb more than ethanol, unlike the results presented here, however the vapour pressures were high and coverage was likely to be greater than monolayer. The authors proposed that as the surface oxygen level increased, the fibre polarity increased thus more polar molecules adsorbed on the surface.

In a work undertaken by Andreu et al., gravimetric adsorption studies on untreated, non-porous, carbon black showed similar trends to those observed in this work on carbon fibre in the adsorption isotherms for methanol, ethanol and isopropanol at low pressures [29]. The isopropanol adsorbed the most on the carbon black while methanol adsorbed the least. At increased pressures, the level of adsorption changed; the methanol showing greater levels of adsorption than the isopropanol. The point of change was approximately at the knee of the isotherm, i.e. the point of monolayer completion. After the monolayer was completed, multilayer formation took place [29]. This furthers the argument that adsorption on the fibres in this study is at monolayer coverage. Carrott et al. examined methanol adsorption on non-porous carbon blacks also gravimetrically [38]. Their results showed between one-in-eight to one-in-four of the surface oxygen atoms were covered depending on the carbon type. This suggests certain types of surface oxygen interact more strongly with the methanol, but specific groups were not investigated [38].

Oxidative dehydrogenation and dehydration has been studied on carbon materials of high surface areas for use as catalysts; such is the case of ethanol on activated carbons [32]. On the unoxidised carbons, only dehydrogenation occurred; the sole product being acetaldehyde. The oxidised carbons showed dehydrogenation and dehydration with ethene, ether, 1,3-butadiene, and ethyl acetate being recorded in addition to acetaldehyde. The level of dehydrogenation taking place increased with increasing oxygen level on the fibre. The unoxidised carbons were mainly basic in nature whereas the oxidised carbons were acidic. Carrasco-Marin et al. concluded that dehydrogenation reactions could occur on acid and basic sites but dehydration could only occur on acid sites and the occurrence would increase with the total acidity of the surface [32]. As stated above, dehydrogenation was observed in this study but dehydration was not. The complexity of the spectra could have masked any dehydration event that took place or, as Carrasco-Marin et al. suggested, water produced from the dehydrogenation reaction (due to the association of the removed hydrogen from the adsorbed alcohol with surface oxygen atoms) could have inhibited the dehydration process [32]. Also the work by Pittman et al. on electrochemically oxidised fibres showed adsorption of toluene, ethanol and ammonia increased with increasing surface oxygen on the fibres [39].

The effect of gas phase polarizability of organic compounds on surface uptake has been studied previously on other surfaces; see for example [30]. The adsorption measurements in this work were conducted close to room temperature where multilayers are not expected to be formed. Moreover because the desorption profile of the series of alcohols was symmetric (indicative of second order desorption), the adsorption of the series of alcohol molecules is likely to be dissociative. This is related to the acidity of the molecules concerned, as acid strength is the measure of how easily a molecule loses its proton. The gas-phase acidity of simple organic molecules has been studied by many groups at the experimental [40–43] and theoretical levels [44,45]. In aqueous solution, the acidity of a molecule is measured by the pK_a scale, and it is known that increasing the alkyl chain of the organic molecules within a functional group decreases the acidity. The reason being the polarizability effect of a particular group in solution is removed due to the solvent molecules, while the inductive effect predominates. The polarizability and inductive effect act in opposite directions. For a series of alcohols, the larger the alkyl group the larger is the charge donation to the functional end of the molecule through induction,

making the O—H bond less acidic. Thus, in solution methanol is more acidic than ethanol and so on. However, the same trend is not observed for organic molecules in the gas phase. The absence of solvent molecules, in the gas phase, results in the domination of the polarizability, and as a consequence the acidity of organic molecules actually increases with increasing alkyl chain length. This is most likely the reason why the surface coverage increases with increasing the number of carbon atoms in the series of alcohols studied in this work.

5. Conclusions

The chemical nature of the surfaces of an untreated, electrochemically treated and UV/O_3 treated carbon fibres was studied by a series of temperature desorption spectroscopy of linear alcohols (C1–C4). Two main factors affected the linear alcohols desorption on the carbon fibre surface: (i) the number of carbon atoms present in the alcohol and (ii) the amount of oxygen present on the surface. (i) The interactions between the alcohols and the fibre surface appear to be mainly influenced by the polarizability of the alcohol molecules in the gas phase with longer chain alcohols behaving more acidic than shorter chains. (ii) Increasing the level of oxygen on the surface of the fibres was shown to increase the level of adsorption of alcohol groups as expected from an acid (the alcohol molecules)–base (the surface oxygen atoms) type of interaction. However the relationship between these two points was found to be more complex. The extent of the increase in alcohol uptake with increasing chain length was found to reduce with increasing oxygen level. This might be due to repulsive interactions which can be linked to preferential oxidation sites of the carbon fibre at step edges and defects. Overall this study has shown the TPD method to be promising for further examinations using organic probe molecules to understand the surface properties of carbon fibres.

Acknowledgements

Susan Osbeck gratefully acknowledges the funding for this project provided by EPSRC (grant EP/E504507/1) and Cytec Engineered Materials Ltd (Wilton, UK). The authors thank EPSRC for proving free access to the TEM/SEM facility at the University of St. Andrews and Dr. Wuzong Zhou and Mr Ross Blackley of the University of St. Andrews for their help with the TEM images. The authors also thank Dr Elizabeth Dawson from the University of Huddersfield for providing the Kr BET data.

References

[1] R.H. Bradley, in: H. Marsh, F. Rodríguez-Reinoso (Eds.), Sciences of Carbon Material, 2000, pp. 485–509.
[2] C. Jones, Composites Science and Technology 42 (1991) 275–298.
[3] S. Ebnesajjad, C.F. Ebnesajjad, Surface Treatment of Materials for Adhesion Bonding, William Andrew Inc., New York, 2006, pp. 77–92.
[4] H. Yuan, C. Wang, S. Zhang, X. Lin, Applied Surface Science 259 (2012) 288–293.
[5] J.-Q. Li, Y.-D. Huang, S.-Y. Fu, L.-H. Yang, H.-t. Qu, G.-s. Wu, Applied Surface Science 256 (2010) 2000–2004.
[6] M.J. Rich, P. Askeland, X. Liang, L. Drzal, Extended Abstracts Carbon 2004 Conference, 11–16th July, Brown University, Rhode Island, USA, 2004.
[7] F. Vautard, S. Ozcan, F. Paulauskas, J.E. Spruiell, H. Meyer, M.J. Lanced, Applied Surface Science 261 (2012) 473–480.
[8] W.P. Hoffman, in: H. Marsh, F. Rodríguez-Reinoso (Eds.), Sciences of Carbon Materials, 2000, pp. 437–483.
[9] P.M.A. Sherwood, Journal of Electron Spectroscopy and Related Phenomena 81 (1996) 319–342.
[10] J. Zhou, Z. Sui, J. Zhu, P. Li, D. Chen, Y.-C. Dai, W.K. Yuan, Carbon 45 (2007) 785–796.
[11] U. Zielke, K.J. Huttinger, W.P. Hoffman, Carbon 34 (1996) 983–998.
[12] G.J.J. de la Puente, J.A. Menéndez, P. Grange, Journal of Analytical and Applied Pyrolysis 43 (1997) 125–138.
[13] G.S. Szymanski, Z. Karpinski, S. Biniak, A. Swiatkowski, Carbon 40 (2002) 2627–2639.
[14] J.P. Boudou, J.I. Paredes, A. Cuesta, A. Martínez-Alonso, J.M.D. Tascón, Carbon 41 (2003) 41–56.
[15] F. Yi, X. Lin, S. Chen, X. Wei, Journal of Porous Materials 16 (2009) 521–526.
[16] M. Popescu, J.P. Joly, J. Carré, C. Danatoiu, Carbon 41 (2003) 739–748.
[17] R. Shekhar, M.A. Barteau, Catalysis Letters 31 (1995) 221–237.
[18] J.W. Medlin, ACS Catalysis 1 (2011) 1284–1297.
[19] H. Idriss, Surface Science Reports 65 (2010) 67–109.
[20] R.L. Guenard, L.C. Fernández-Torres, B. Kim, S.S. Perry, P. Frantz, S.V. Didziulis, Surface Science 515 (2002) 103–116.
[21] A.M. Nadeem, G.I.N. Waterhouse, H. Idriss, Catalysis Today 182 (2012) 16–24.
[22] H. Idriss, M.A. Barteau, Advances in Catalysis 45 (2000) 261–331.
[23] S. Osbeck, R.H. Bradley, C. Liu, H. Idriss, S. Ward, Carbon 49 (2011) 4322–4330.
[24] NIST Mass Spec Data Center, S.E.D., Stein, Mass spectra, in: P.J. Linstrom, W.G. Mallard (Eds.), NIST Chemistry Webbook, NIST Standard Reference Database Number 69, National Institute of Standards and Technology, Available from: http://webbook.nist.gov (accessed 23.09.10).
[25] E.I. Ko, J.B. Benziger, R.J. Madix, Journal of Catalysis 62 (1980) 264–274.
[26] R.J. Diefendorf, E. Tokarsky, Polymer Engineering and Science 15 (1975) 150–159.
[27] Y. Xie, P.M.A. Sherwood, Chemistry of Materials 2 (1990) 293–299.
[28] H. Idriss, E.G. Seebauer, Journal of Molecular Catalysis A: Chemical 152 (2000) 201–212.
[29] A. Andreu, H.F. Stoeckli, R.H. Bradley, Carbon 45 (2007) 1854–1864.
[30] S.V. Chong, H. Idriss, Surface Science 504 (2002) 145–158.
[31] D.R. Lide, CRC Handbook of Chemistry and Physics, 73rd ed., CRC Press Inc., Florida, USA, 1992, pp. 10-193–10-202.
[32] F. Carrasco-Marin, A. Mueden, C. Moreno-Castilla, Journal of Physical Chemistry B 102 (1998) 9239–9244.
[33] C.A. Leon y Leon, J.M. Solar, V. Calemma, L.R. Radovic, Carbon 30 (1992) 797–811.
[34] E. Farfan-Arribas, R.J. Madix, Journal of Physical Chemistry B 106 (2002) 10680–10692.
[35] M.A. Nadeem, G.I.W. Waterhouse, H. Idriss, Catalysis Today 182 (2012) 16–24.
[36] M.A. Nadeem, J.M.R. Muir, J.B. Metson, H. Idriss, Physical Chemistry Chemical Physics 13 (2011) 7637–7643.
[37] H. Idriss, M.A. Barteau, Journal of Physical Chemistry 96 (1992) 3382–3388.
[38] P.J.M. Carrott, M.M.L.R. Carrott, I.P.P. Cansado, Carbon 39 (2001) 193–200.
[39] C.U. Pittman, W. Jiang, Z.R. Yue, S. Gardner, L. Wang, H. Toghiani, C.A. Leon y Leon, Carbon 37 (1999) 1797–1807.
[40] J.B. Cumming, P. Kabarle, Canadian Journal of Chemistry 56 (1978) 1–9.
[41] R. Yamdagni, P. Kebarle, Journal of the American Chemical Society 95 (1973) 4050–4052.
[42] J.L. Brauman, L.K. Blair, Journal of the American Chemical Society 93 (1971) 4315–4316.
[43] K. Hiraoka, R. Yamdagni, P. Kebarle, Journal of the American Chemical Society 95 (1973) 6833–6835.
[44] J. Catalàn, Journal of Physical Organic Chemistry 9 (1996) 652–660.
[45] I.A. Topol, G.J. Tawa, R.A. Caldwell, M.A. Eissenstat, S.K. Burt, Journal of Physical Chemistry A 104 (2000) 9619–9624.